ELSEVIER

Catalysis Today 52 (1999) 235–247

CATALYSIS TODAY

www.elsevier.com/locate/cattod

Modelling of catalytic gas–solid fluidised bed reactors

L. Marmo, G. Rovero, G. Baldi*

Dipartimento di Scienza dei Materiali e Ingegneria Chimica, Politecnico di Torino, C.so Duca degli Abruzzi 24, 10129, Torino, Italy

Abstract

Flow regimes in gas–solid fluidisation are presented on a broad scale from captive smooth fluidisation to dilute transport. The parameters useful to identify each transition are critically presented. The description of catalytic gas–solid fluidised beds is considered starting from simplified two-phase models; a third phase given by clouds and wakes is then introduced to justify their effect in promoting solids circulation. Different hydrodynamic features have been used in the literature to describe the dense and the dilute phase, according to the mixing effect of bubbles.

Circulating fluidised bed modelling is approached according to the definition of a hydrodynamic regime. The numerous models appearing up to now in literature are presented, from earlier homogeneous models to the latest continuous radial profile and clustering models.

The development of spouted beds as chemical reactors is given from the first fundamental approach, followed by the experimentation in the late 1970s, ending with more complex descriptions that take into account all the spouted bed zones.

A concluding chapter on model selection offers general criteria to tackle the mathematical description which predicts the performance of catalytic reactors in the different regimes.

Keywords: Gas–solid fluidisation; Fluidised bed reactors; Two-phase models

1. Introduction

The development and the current importance of fluidised bed processes in the world is closely connected to the fuel industry. Since the late 1950s, the interest in fluidisation shown by the scientific community reached a considerable level of importance, which resulted in a massive production of papers and books. At first, low velocity processes, such as bubbling fluidised bed processes, spouted beds, turbulent beds and finally circulating fluidised beds, were studied with more frequency. Fluid-catalytic cracking, combustion, partial oxidations (phthalic anhydride for example) represents some of the more common processes carried out in a fluidised reactor. Books and complete reviews by a number of authors were published: the classical book by Kunii and Levenspiel [1], and more recently, one by Grace et al. [2] are recommended. Hence, it is not the aim of this paper to revise the development of fluidised bed reactors modelling, nevertheless, the field of fast beds is undergoing a quick evolution, and modelling of these reactors is not sufficient yet. As far as the modelling of bubbling reactors is concerned, a number of models based on two-phase theory of fluidisation were proposed and validated in a range of laboratory and industrial conditions. An overview will be given on this aspect.

*Corresponding author.
E-mail address: gbaldi@athena.polito.it (G. Baldi)

0920-5861/99/$ – see front matter
PII: S0920-5861(99)00078-4

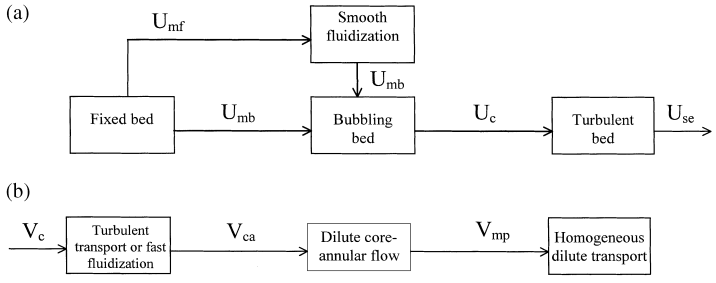

Fig. 1. Flow regimes in gas–solid fluidisation.

2. Flow regimes in gas–solid fluidisation

Gas–solid fuidisation regimes depend on particle properties [3], reactor geometry and gas velocity. Fluidisation regimes can be divided into non-captive and captive regimes, depending on whether a significant amount of particles are entrained out of the vessel and therefore need to be reintroduced. In a non-captive regime the solid circulation rate becomes a variable. Flow regimes for captive fluidisation are depicted in Fig. 1(a), and for non-captive in Fig. 1(b).

By increasing the gas flow rate through a bed of particles, different conditions of fluidisation arise. At a gas velocity higher than the minimum bubbling velocity U_{mb}, the gas is bubbling in an ebullieted bed. Only Geldart A particles undergo smooth fluidisation and for them $U_{mf}<U_{mb}$. In bubbling beds the dense phase is continuous (emulsion), and a significant part of the gas passes through the bed in the form of dispersed bubbles; the bed surface is easily observable. By increasing the gas velocity, pressure fluctuations inside the bed reach a maximum when the following relationship is satisfied [4]:

$$Re_{tc} = 1.24Ar^{0.45}. \quad (1)$$

The corresponding velocity U_{tc} is considered to define the onset of turbulent fluidisation, which is characterised by bubble splitting at a high frequency, to the point at which the bubbles cannot be individually recognised anymore. The turbulent bed can be described as a two-phase system with short time transitional nature: voids and clusters of solids become alternatively continuous and discontinuous phases at high frequency: turbulent beds do not show a neat surface at the top anymore. The space above bubbling and turbulent beds, called freeboard, is characterised by a very low, exponentially decaying, solid hold-up. Captive regimes are commonly considered to exist up to the velocity U_{se} at which the "onset of significant elutriation" is observed [5]:

$$Re_{se} = 1.53Ar^{0.5}. \quad (2)$$

Non-captive regimes are characterised by gas velocity and a net solid flux G_s, hence the transition velocity should be defined by both parameters. A formulation is proposed according to the general relationship [5]:

$$V_i = U_i + \frac{G_s \epsilon_i}{\rho_p(1-\epsilon_i)}. \quad (3)$$

Practical non-captive regimes have been depicted in Fig. 1(b); on the basis of Eq. (3) the velocity that denotes the onset of turbulent flow or fast fluidisation is

$$V_{tc} = U_{tc} + \frac{G_s \epsilon_{tc}}{\rho_p(1-\epsilon_{tc})}. \quad (4)$$

Methods for estimating ϵ_{tc} are given in [6].

Generally, the lower boundary of fast fluidisation regime operation is not given by Eq. (4) but by type B or C choking phenomena that can persist at velocities higher than V_{tc}. A prediction can be made according to [7]. Fast fluidisation is the regime at which circulating fluidised beds are often operated. It is characterised by strong axial and radial gradients of solid concentration, gas velocity and solid flux; a dense bottom region and a dilute top region with exponentially decaying hold-up are observed; core-annulus structures are commonly present. The upper limit to the fast fluidisation regime is given by the "type A choking velocity

transition'' as defined in [5] according to Eq. (3):

$$V_{ca} = U_{se} + \frac{G_s \epsilon_{ca}}{\rho_p (1 - \epsilon_{ca})}. \quad (5)$$

Guidelines for calculation of ϵ_{ca} are found in [4,6]. At $U > V_{ca}$ the dilute core-annular flow is attained: the axial hold-up profile is very smooth but radial gradients still exists. When $U > V_{mp}$, ''minimum pressure drop velocity'', Eq. (6)[8], the homogeneous dilute transport regime is reached and almost no axial solid concentration gradients and reduced radial gradients are observed.

$$V_{mp} = 10.01 (g d_p)^{0.347} \left(\frac{G_s}{\rho_g}\right)^{0.310} \left(\frac{d_p}{d}\right)^{-0.139} Ar^{-0.021}. \quad (6)$$

Regime maps can be found in [4].

A particular case of fluidisation that of spouting. Spouted beds can be viewed as beds in which a jet of gas at high velocity enters the bed bottom and extends upwards to the upper free surface. This produces a fountain of solids and vigorous internal circulation of particles that travel down the annulus between the jet and the walls of the reactor.

3. Models for bubbling fluidised bed reactors

Prediction of the bed performance of a catalytic reactor requires knowing how the gas passes through the bed. Due to the complex hydrodynamics, the basic reactor models, plug flow and perfect backmix, do not hold since the gas presents a certain degree of bypass in the dilute phase and recirculation within the dense phase: the overall conversion is affected to a different extent by the gas repartition. An early description [9] introduced a two-phase model (i.e. a rising bubble phase and a stagnant emulsion at minimum fluidizing conditions); many authors [10–15] later improved it. Based on this simple assumption gas mass transfer can follow two mechanisms: a direct interchange from bubble to the emulsion bulk (and vice versa) or a two-step transfer from the bubble to the dense phase through the cloud. In order to clarify the mechanism to be considered, gas paths inside the bubble must be examined: gas enters the bubble from the bottom, where pressure is lower, and leaves from the top. In Geldart A particle beds, bubbles undergo frequent splitting and coalescing (see [15] for more details) and rise with velocity much higher than U_e, which is close to U_{mf}. Gas that has left the bubble top into the emulsion rises slower than bubbles, it is then overtaken and re-enters the bubble from the bottom. This closed-loop circulation gives origin to a very thin cloud. In the case of Geldart B particles, U_e is of the same order of U_b, hence each rising bubble takes longer to re-capture the gas permeated in the dense phase: the cloud in this case is larger. In Geldart D particle beds, U_e commonly exceeds U_b and the gas uses the bubbles as bypass: no loop circulation occurs and no cloud can be identified. In beds of Geldart A and B solids, a tail (the wake) of solids transported upward follows bubbles. The initial assumption of constant voidage and gas velocity in the emulsion ($U_e = U_{mf} = \text{const}$) was modified with two distinct correlations for the Geldart A and AB solids [16], Eq. (7) and for the Geldart B and D solids (Eq. (8)):

$$(\epsilon_e/\epsilon_{mf})^3 [(1 - \epsilon_{mf})/1 - \epsilon_e] = (u_e/U_{mf})^{0.7}, \quad (7)$$

$$\frac{U_e - U_{mf}}{U - U_{mf}} = 1/3. \quad (8)$$

Werther [17] came up with a bubble rise velocity correlation covering the whole range of fluidisation regimes with an equation

$$U_b = \psi (U - U_{mf}) + \alpha U_{br}, \quad (9)$$

ψ being the fraction of gas flow rate passing in the form of bubbles, and α a coefficient depending on the bed diameter as reported in the literature. It is worthwhile noting that A and B particles have a non-similar effect on the $(U - U_{mf})$ term. The volumetric fraction of bubbles in the bed can be expressed by several different correlations depending on bubble velocity:

slow bubbles

$$(U_b \leq U_e)\delta = (U - U_{mf})/(U_b + 2U_{mf}), \quad (10)$$

intermediate bubbles $\delta = (U - U_{mf})/(U_b + U_{mf})$

or $\delta = (U - U_{mf})/U_b$, (11)

fast bubbles $(U_b \geq 5U_{mf}/\epsilon_{mf})\delta$

$= (U - U_{mf})/(U_b - U_{mf})$. (12)

Moreover, cloud and wake volumes can be related to bubble volume according to analytical or graphical

correlations. The volume of solids in the three regions, referred to as the bubbles volume, can be related by a mass balance over the whole bed

$$\delta(\gamma_b + \gamma_{cl} + \gamma_e) = (1 - \epsilon_f) = (1 - \epsilon_{mf}) \cdot (1 - \delta). \quad (13)$$

By increasing the gas velocity, bubble wakes induce an increased emulsion circulation, which drags the gas down; such gas backflow begins at

$$U/U_{mf} = 6 \text{ to } 20. \quad (14)$$

At these conditions backmixing is required to be accounted for, for gas conversion modelling.

The gas interchange between bubble and emulsion can be seen as a direct step process in case of slow bubbles (absence of cloud). Alternatively, with fast clouded bubbles, the gas interchange process occurs in a two-step series; the overall mass transfer coefficient is expressed by

$$1/K_{be} = 1/K_{bc} + 1/K_{ce}. \quad (15)$$

Usually, these coefficients are defined per unit volume of bubble. Alternatively, mass transfer coefficients may be used as related to the specific interphase area. Experimental findings for non-adsorbed gases are summarised [1] as a function of: bubble diameter, gas velocity, bed diameter, adsorbed gas show gas interchange one order of magnitude higher. In the case of fine particles K_{bc} and K_{ce} can be calculated according to

$$K_{bc} = 4.5(U_{mf} \cdot d_b^{-1}) + (\mathscr{D}^{1/2} g^{1/4} d_b^{-5/4}), \quad (16)$$

$$K_{ce} = 6.77(\mathscr{D} \epsilon_{mf} U_{br} d_b^{-3})^{1/2}. \quad (17)$$

Much attention is given in the literature to the fact that fluidised beds need more catalyst than fixed bed reactors: a quite complete list of experimental studies is presented [1]. A number of models have been proposed to compare the experimental data and to predict the conversion in large units [18–26]. Modelling of fluidised bed reactors may follow three routes:

(a) a two-phase description with the excess of gas flowing as bubbles,

(b) an overall description of single-phase or two-phase reactors with axial gas dispersion in the emulsion phase, and

(c) a physical description, the so-called hydrodynamical description, originated by the fundamental work by Davidson and Harrison [10], which provides the gas streamline field inside and around the bubbles: the latter approach gives a sound basis for rational scale-up.

The first attempts, according to the (a) method, assumed different hydrodynamics in the dense phase and/or different descriptions for the gas interchange. The second approach needs the determination of a dispersion coefficient: by reviewing the published data it is quite safe to assume that the gas behaves more like an ideal plug in large units and with coarse particles. The third method has been far more successful and makes use of two or three phases, depending on whether the cloud is considered independently. Again bubbles are solid-free or the effect of a very lean suspension is taken into account (detailed review is given in [1,27]). For a first-order reaction material balances in a bubble, cloud and emulsion, are:

$$U_b \frac{dC_b}{dz} = -C_b \gamma_b k_r - K_{bc}(C_b - C_{cl}), \quad (18)$$

$$U_e \frac{dC_e}{dz} - C_e \gamma_e k_r + K_{ce}(C_{cl} - C_e), \quad (19)$$

$$0 = C_{cl} \gamma_{cl} k_r + K_{ce}(C_{cl} - C_e) - K_{bc}(C_b - C_{cl}). \quad (20)$$

In a number of cases $U_b \gg U_e$ so that the flow in the emulsion is neglected; in other cases no reaction is considered to take place within the bubbles due to the negligible solids concentration. Other models do not include the cloud-wake phase and the gas interchange is direct between bubbles and emulsion (K_{be} in Eqs. (18) and (19)). Some models, then, [28] do include the downflow of gas which occurs for A and AB particles operated at a gas velocity far exceeding U_{mf}. By maintaining the bubbles in plug flow, the emulsion is conveniently described with a certain axial dispersion by including a dispersion term such as

$$\mathscr{D}_l = \frac{dC_e^2}{dz^2} - U_e \frac{dC_e}{dz} = C_e \gamma_e k_r - K_{ce}(C_{cl} - C_e). \quad (21)$$

The so-called ‘‘bubble assemblage model’’, consisting in well-mixed slices of fluidised beds was proposed [11] to produce, in practice, an overall plug flow description, depending on bubble-to-bed diameter ratio. Complete mixing can be accounted for in the emulsion for vigorous bubbling which encourages regular patterns of solids recirculation

typical of B solids in large units. In this case it is possible to write

$$-(C_{e,out}-C_{e,in})=\gamma_e C_{e,out}k_r\tau_e - K_{be}(C_{b,out} - C_{e,out})\tau_e. \quad (22)$$

Also, the bubble phase can be written as a perfectly mixed system

$$-(C_{b,out}-C_{b,in})=\gamma_b C_{b,out}k_r\tau_b + K_{be}(C_{b,out} - C_{e,out})\tau_b \quad (23)$$

considering, in this case, a direct bubble–emulsion gas interchange. Such a hydrodynamical assumption is sound for staged fluidised beds where the bubble life-time is shortened in each sector since the bed height can be considerably smaller than the one of conventional units. The entrance zone may be viewed as a true jet region with some particle entrainment [29] or alternatively as a sequence of bubbles frequently coalescing and forming again. Such evidence leads to an entrance region model [30] characterised by a higher mass transfer rate between phases than in the bed, which should be considered. A contact model for the freeboard was added [31] to account for the decaying particle concentration before a complete gas–solids separation. The scale-up of fluidised beds is known to be more difficult than that of other types of reactors [32]: successful examples were reported [1], as well as failures [33,34]. A detailed analysis on scale-up modelling was given in [15], where a two-phase model applied to fine particles (type A and B) was considered, with simplification for the gas hydrodynamics: ideal plug flow in both solid-free bubble and emulsion phases and no reaction in the freeboard. Geometrical variations to the bed were introduced: enlargement, height, distributor design, bed sectioning generated by baffle insertion, bubble diameter variation with distance from distributor and particle size distribution. Generally, it is possible to say that conversion decreases due to the installation of coarser distributors in larger units which form bigger bubbles with a reduced specific mass transfer area. Internals are useful to limit the bubble growth and to redistribute the gas in the dense phase; optimal design is required in order not to abnormally increase the overall freeboard volume and therefore the reactor volume. Reactor models conceived for first-order kinetics can be extended to complex reaction paths typical of industrial production. Examples of application of the models studied for industrial cases have been presented [1,21,35,36].

4. Models for turbulent beds

In turbulent beds, aggregates (either suspension or clusters) show a transitional nature that results in an almost null gas bypass as occurs in bubbling fluidisation and in an enhanced gas transfer between phases: improved conversion was generally observed [37] compared to bubbling beds. Conversion in turbulent beds lays between what predicted from plug flow and CSTR models. A common approach to dense phase modelling consists in assuming [37–41] axial dispersion coefficients which can result in being lower than in the case of bubbling beds [39,40]. Examples of longitudinal dispersion coefficients are given, respectively, in Eqs. (24) and (25) [40,42]:

$$Pe = 7 \cdot 10^{-2} Ar^{0.32}(d_p/d)^{-0.4}, \quad (24)$$

$$\mathscr{D}_l = 0.1835 \cdot \epsilon^{-4.4453}. \quad (25)$$

The two correlations provide rather different longitudinal dispersion, with Peclet number close to 2 and 8, respectively. The results are consistent with previous findings.

Axially dispersed models can be written in the form

$$\mathscr{D}_l \frac{d^2 C_g}{dz^2} - U\frac{dC_g}{dz} = C_g(1-\epsilon)\cdot k_r. \quad (26)$$

Evidence of radial disuniformities in solids hold-up [43] and strong local heterogeneity in the suspension density are so evident that some authors [44] refer to this bed as a turbulent bed of clusters. Two-zone models, taking into account dense and lean phase and interphase gas transfer, were suggested [37] and depicted [45]. Further examples of two-zone modelling are available in [40,46]. Freeboard of turbulent beds can be handled as a plug flow with a contact efficiency parameter [13,47].

5. Models for circulating fluidised bed reactor

Due to geometrical features and high gas velocity, the initial description of CFBR modelling was closely

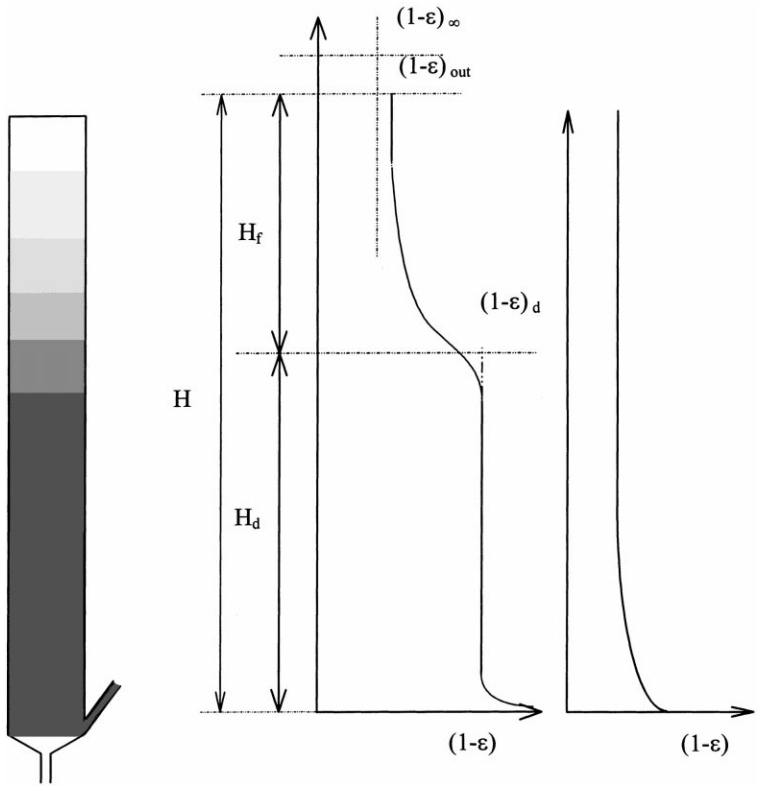

Fig. 2. Hold-up profile in the riser of a CFB.

related to plug flow systems. Qualitative longitudinal solids hold-up profiles for fast fluidisation and pneumatic transport are depicted in Fig. 2(a) and (b), respectively. Criteria for calculating the height of the bottom dense zone H_d are given in [45,48]. If $U>V_{ca}$, the acceleration section is followed by a fully developed zone, where hold-up is almost constant and the slip factor Ψ (gas to solid actual velocity ratio) approaches 2. On the basis of a wide range of experimental data, an estimation is proposed according to [49]:

$$\frac{U(1-\epsilon)\rho_s}{\epsilon G_s} = \Psi = 1 + \frac{5.6}{Fr} + 0.47 \cdot Fr_t^{0.41}. \quad (27)$$

Reviews [50,51] on CFB hydrodynamics were given; the latter emphasises the distinction between type I, II and III models given by [52], depending on whether hold-up profiles are taken into account. As summarised by Grace and Lim [53], the models presented for CFB reactors correspond roughly to the following classification.

5.1. Type I models: axial hold-up profiles models

Many authors [45,54–62] adopt flat radial gas and solids profiles. A simple plug flow in the gas phase was demonstrated to predict [57] ozone concentration decay at low conversion only. Ozone conversion in a 0.102 m diameter riser with and without baffles was explored [56] by a plug flow model. Mass transfer resistance between the bulk of the gas and the particle surface was accounted for by introducing a contact efficiency parameter, already suggested [63], which was assumed to be the ratio between the active and the total catalyst area. The efficiency was found to range between 0.4 and 0.7, increasing with gas velocity. Such a model was conceived as being

$$U\frac{dC_g}{dz} + k_s a_s \eta(1-\epsilon)\cdot(C_g - C_s) = 0, \quad (28)$$

$$k_s a_s (C_g - C_s) = k_r C_s \alpha, \quad (29)$$

for the gas and the solid phases, respectively, with α being the effectiveness factor for porous particles. Kunii

and Levenspiel [45], according to their hydrodynamic model [64], proposed to consider a dense region at the bottom upstream of a lean phase. The latter is described using plug flow and contact efficiency by

$$U\frac{dC_g}{dz} + k_r\eta(1-\epsilon)\cdot C_g = 0, \quad (30)$$

where the contact efficiency is given by [65]:

$$\eta = 1-(1-\eta_d)\cdot e^{-bh} \quad (31)$$

in the lean zone of fast beds and η=1 for pneumatic transport. In other models [59,60] a perfect contact was assumed: both models overestimated conversion since a contact efficiency between 0.3 and 1 would be needed (though the latter model considers longitudinal dispersion calculated according to [29]). The effect of particle dimension on the contact efficiency parameter was demonstrated in [66].

5.2. Type II models: consider the radial structure

5.2.1. Core-annulus models

Radial profiles of phisical properties in CFB are simplified according to a core-annulus (CA) structure. The flow structure reported in Fig. 3 was proposed [67,68] to account for solids downflow at the wall: a lean central zone (core) is surrounded by a dense annulus where gas and solids can be exchanged. Typical model expressions are:

$$U_c\frac{dC_c}{dz}(1-\epsilon_c)k_rC_c + 2\frac{k_g}{r_c}(C_c - C_a) = 0, \quad (32)$$

$$U_a\frac{dC_a}{dz} + (1-\epsilon_a)k_rC_a - 2\frac{k_g}{r_c}(C_c - C_a) = 0. \quad (33)$$

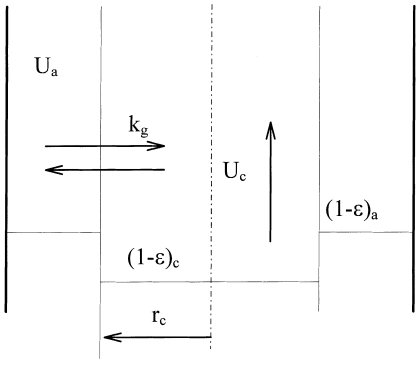

Fig. 3. Scheme of the core-annulus structure.

Voidage in the core and in the annulus must satisfy the volumetric mass balance

$$(1-\epsilon_c)r_c^2 + (1-\epsilon_a)\cdot(R^2 - r_c^2) = (1-\epsilon)R^2. \quad (34)$$

Some authors investigated core-annulus model effectiveness in predicting gas RTD curves [69,70], CFBR performance [58–60,71–73] or its potential applications [61,74–76]. These models differ basically in the parameter settings: stagnant gas in the annulus [60,69–73], or alternatively, gas backflow [59,61,74] were assumed. Modifications are available to evaluate the core radius: on the basis of gas RTD measurements, Patience and Chaouki [70] proposed

$$\left(\frac{r_c}{R}\right)^2 = \frac{1}{1+1.1Fr(U_p/U)^{0.083Fr}}. \quad (35)$$

Werther [77], as a measure of the ''fluid mechanical wall zone'' extending from the wall to the point where null local solid flux is measured, proposed

$$\frac{d_t/2 - r_c}{d_t} = 0.55Re_t^{-0.22}\left(\frac{H}{d_t}\right)^{0.21}\left(\frac{H-h}{H}\right)^{0.73}. \quad (36)$$

Some authors assumed Eq. (35)[60], others Eq. (36)[61,74]. Core radius was also left as model parameter [73], or devised from a shear stress balance at the boundary between core and annulus [75]. In general, core radius is found to range from 90% to 99% of the riser radius, it increases with U_g and decreases as G_s increases; in [73] conversion data was fitted by means of ratios as low as 80%.

The following correlation [70] used to account for gas transfer coefficient can be obtained

$$Sh_c = k_g d(r_c/R)/\mathscr{D} = 0.25Sc^{0.5}Re_c^{0.75}(U_p/U)^{0.25}. \quad (37)$$

Such a correlation, yielding values ranging around 0.05 m s^{-1}, was adopted in [60]; other authors assumed similar or slightly lower values [59], though their models overestimated the conversion. Some authors left the gas transfer coefficient as model parameter [71,75]. Null gas transfer was also assumed [73], resulting in a thick annulus. In one case [78] literature data was fitted without the help of any contact efficiency parameter, yielding much lower gas transfer coefficients with respect to Eq. (37). In the light of these works, the core-annulus approach

seems to need at least one fitting parameter. Suitability for scale-up is still under discussion.

5.2.2. Continuous radial profiles models

The core-annulus approach cannot be considered fully comprehensive of the suspension hydrodynamics: a number of examples of continuous change in properties values occurring in the radial direction have appeared in the literature. Two correlations for the radial hold-up profile were proposed, respectively, [79,80]:

$$\epsilon(r) = \epsilon_{\mathrm{av}}^{(0.191+(r/R)^{2.5}+3(r/R)^{11})}, \tag{38}$$

$$\epsilon(r) = -(1-\epsilon_{\mathrm{av}})\beta'(r/R)^2 + \epsilon_{\mathrm{av}} + \frac{\beta'}{2}(1-\epsilon_{\mathrm{av}})\beta' = 1.3 \text{ to } 1.9. \tag{39}$$

Many authors [80,81] measured solids flux profiles: the correlation for the radial profile given by [80] is

$$\frac{G_{\mathrm{s}}(r)}{G_{\mathrm{s}}} = a\left[1-\left(\frac{r}{R}\right)^m\right] + 1 - \frac{ma}{m+2}. \tag{40}$$

Radial gas velocity profiles were measured [82,83] by injecting a tracer in the riser

$$U(r) = U\left(\frac{3n+1}{n+1}\right)\left(1-\left(\frac{r}{R}\right)^{(n+1/n)}\right). \tag{41}$$

All these correlations contain a number of adjustable parameters (m, a, β, n) whose average values cannot be identified yet. Radial gas dispersion results are, up to now, quite contradictory: an increase [83,84], negligible influence [85,86] or a decrease [87,88] with G_{s} was reported. The gas velocity was demonstrated to increase the radial dispersion $\mathscr{D}_{\mathrm{r}}$ according to [87], an opposite effect was shown [84,88], too. The two available correlations [84,88] were revised and a new one was proposed [89]. On this basis a few models were originated to account for the radial variation of properties. Such radial profiles can be described as a continuous change of suspension properties [61,90], or as a rising lean phase and dense clusters which give different radial hold-up profiles [91–93]. A model, which takes into account the radial gas velocity profiles according to Eq. (41), a radial dispersion from [83], axial and radial profiles for solids hold-up, was developed [90]. No simultaneous flow of a dense and a lean phase or a sharp boundary between bottom and upstream zone were needed. Such a description, combined with a complex kinetic scheme for FCC cracking, was successfully applied to a 1 m diameter circulating cracking unit: excellent agreement was obtained for gasoline yield. The model formulation, as far as the gaseous reactant is concerned, is

$$\frac{\partial(U(r)C_{\mathrm{g}}(r))}{\partial z} = \frac{\mathscr{D}_r}{r}\frac{\partial}{\partial r}\left(r\frac{\partial C_{\mathrm{g}}(r)}{\partial r}\right) + R(r)_{\mathrm{g}}. \tag{42}$$

A two-zone model was applied to the fully developed zone of a 0.4 m diameter riser [91], where concentration of the lean and the dense phases were constant with radius and where gas and solid velocities were calculated from [81]. Radial gas dispersion in the lean phase was considered with a gas transfer coefficient between clusters and lean phase of K=0.3 s^{-1}.

5.3. Type III models: based on fundamental equations

A number of models for two-phase gas–solid flows have been published up to now, based on continuity, momentum and energy equations; extensive reviews are provided [94,95]. Chemical kinetics were also assembled [96] to describe a commercial combustor.

6. Bottom zone modelling

Since the bottom zone hydrodynamics are strongly affected by solids acceleration due to the fact that flat axial reactant profiles were observed [57,71,73], some authors assumed complete axial gas backmixing [60,91,92,97] at a certain elevation in the riser. The length of the mixed zone, ranging between approximately 0.5 and 1 m, was left as a parameter in [60]. Alternatively [97], the primary zone of the combustor model was assumed to behave as two CSTRS in series with some mass transfer resistance. Some authors [91] divided the bottom zone into two concentric sections, both perfectly mixed along the axial direction. In the inner zone they assumed $\mathscr{D}_{\mathrm{r}}=\infty$, while assuming $\mathscr{D}_{\mathrm{r}}=0$ in the external one. In a previous model [98,99] two consecutive zones were assumed: a bubbling bed reactor followed by a short and perfectly mixed section corresponding to the splash zone. On the contrary, a dense and lean plug flow zone model, with a certain gas mass transfer, was also suggested

[45], according to Eq. (43):

$$\ln\frac{C_{g,in}}{C_{g,out}}=\left[k_r(1-\epsilon_l)+\frac{1}{(1+\partial_d K_{dl})+1/k_r(1-\epsilon_d)}\right]\frac{H_d}{U}. \quad (43)$$

7. Spouted beds as chemical reactors

A spouted bed can be viewed as a special case of fluidisation in which the jet region extends up to the upper free surface of the bed. The spout and annulus zone have such a different gas–solid contacting that they were described distinctly since the first approach as chemical reactor modelling [100]. The spout zone acts as a dilute transport system, the peripheral annulus has many similarities with a countercurrent downflow bed, the major peculiarities being a progressive gas percolation into the bed from the spout. Isothermal modelling was then tackled [101] to compare experimental data; subsequent validation of a streamline description of the annulus was given [102] by scale-up experimentation. The hydrodynamical description may affect considerably the performance of the reactor in the case of gas distribution differing from the basic one (the gas flow rate exceeding the minimum spouting condition passes through the spout in a similar way as the bubble receive the excess of minimum fluidisation). An alternative approach for gas phase distribution was provided in [103]. The one-dimensional model was modified [104] by introducing thermal effects in an adiabatic reactor with limitations originated by lumping of fluid and particle energy balances. By introducing the fountain as plug flow and the annulus as a bi-dimensional approach, a complex description with Ergun's equation for the gas phase was given [105].

8. Model selection

The description of bubbling beds should be restricted to medium size or large units where bubbles may play an overall mixing effect on solids circulation: from this point of view particle size and fluid flow rate must be considered.

D particles are seldom fluidised because they give origin to slugging or spouting; in conventional fluidisation the gas flows as plug both in the bubble phase (used as gas bypass) and in the dense phase. The flow partition is quite neat and a mass transfer coefficient between the phases, based on convective gas flux, must be taken into account.

A Geldart particles give rise to almost negligible gas rates in the emulsion (since it is characterised by low permeability) where the fluid is in plug flow with some optional axial dispersion. Due to the quite clear hydrodynamics, only two-phase models should be considered, with the lean phase flowing as a piston with relevant mass transfer to the dense phase due to both a mass transfer coefficient as well as to convective flow originated by frequent bubble coalescing and splitting.

B particles lead typically to three phases while they undergo fluidisation, the third phase being composed of the cloud/wakes that accompany each bubble in its upward travel, this feature has to be taken into account in modelling mass transfer between bubble to emulsion, through the cloud. Since beds are operated at velocities largely exceeding minimum fluidisation, the mixing effect in the emulsion is important, i.e. this hydrodynamical condition is modelled. Bubbles are maintained in plug flow. The effect of the freeboard is generally moderate: the particle load decays exponentially and the total hold-up is negligible if compared to the upstream region. A similar geometrical consideration can be extended to the entrance zone, which is generally relatively small in industrial units. Since jetting enhances phase transfer, multistaged fluidisation should consider the effect of these zones.

Modelling of CFB as a chemical reactor is at the moment evolving rather quickly, so that modelling assumptions are still subject to change, although, rough indications can be given on the basis of flow regimes. The almost uniform solids suspension suggests that pneumatic transport regime can be modelled by assuming plug flow for the gas phase and a contact efficiency to account for low conversions [56,59,60]. Further experimental work is needed to assess whether gas mixing needs to be accounted for at the bottom and where the boundary between the two zones is located.

The fast fluidisation regime is suitably modelled by assuming continuous gas velocity radial profiles [82,90], hold-up and flux of solids varying with radius [79,83]. According to a recent paper [90], no axial dispersion is needed for the gas phase in the fully

developed flow, a very low radial dispersion coefficient ($\approx$0.03 $m^2\ s^{-1}$) seems to be an optimal choice.

Models concerning lean rising and dense refluxing phases, such as in [91], are very promising but still contain parameters; therefore they need to be tested against actual kinetics in order to be fully accepted. The bottom of a fast fluidised bed, extending up to the end of the dense zone, should be considered to be perfectly mixed with respect to the gas phase [60,91].

Turbulent beds are conveniently described as plug flow reactors with a certain longitudinal dispersion. Only in the case of very fast reactions compared to mass transfer phenomena, a two-zone model (lean phase and clusters) with enhanced mass transfer [40] should be considered.

As far as spouted beds are concerned, it is well assessed that axisymmetric models give the best description at the present time. Since heat losses can be easily controlled and by considering that the moderate temperature processes (such as drying of coarse solids) are probably the most interesting in such apparatuses, an adiabatic description makes sense. In this view, a sound reference can be found in [104], since it includes all of the three constituting regions (annulus, spout and fountain) and thanks to its full predictivity.

9. Nomenclature

Ar	Archimede number, $\rho_g(\rho_p-\rho_g)d_p^3 g/\mu_g^2$ (dimensionless)
a_s	catalyst specific surface (m^{-1})
b	decaying coefficient, Eq. (31) (m^{-1})
C	concentration (mol m^{-3})
d	vessel column diameter (m)
d_p	particle diameter (m)
$\mathscr{D}$	gas diffusivity ($m^2\ s^{-1}$)
$\mathscr{D}_l$	longitudinal gas dispersion ($m^2\ s^{-1}$)
$\mathscr{D}_r$	radial gas dispersion (dimensionless)
d_t	hydraulic diameter (m)
Fr	Froude number, $U_g/(gd)^{0.5}$ (dimensionless)
Fr_t	particle Froude number, $U_t/(gd)^{0.5}$ (dimensionless)
G_s	solids flux (kg $m^{-2}\ s^{-1}$)
h	axial location (m)
H	vessel column height (m)
K_g	gas exchange coefficient (s^{-1})
k_g	core-annulus gas exchange coefficient ($m\ s^{-1}$)
k_r	intrinsic chemical kinetic (s^{-1})
k_s	gas to particle mass transfer coefficient ($m\ s^{-1}$)
Pe	Peclet number, $UH/\mathscr{D}_l$ (dimensionless)
Pe_r	radial Peclet number, $UR/\mathscr{D}_r$ (dimensionless)
r	radial position (m)
R	column vessel radius (dimensionless)
Re_c	core Reynolds number, $U\rho_g d/\mu(r_c/R)^{0.5}$
Re_m	modified Reynolds number, $(G_s/U\rho_g)d/\mu$ (dimensionless)
Re_p	particle Reynolds number, $U\rho_g d_p/\mu$ (dimensionless)
Re_t	Reynold number based on hydraulic diameter, Ud_t/ν (dimensionless)
R_g	reaction rates in gas phase, Eq. (42) (mol $m^{-3}\ s^{-1}$)
R_t	hydraulic radius (m)
Sc	Schmidt number, $\mu/\mathscr{D}\rho_g$ (dimensionless)
Sh_c	modified Sherwood number (dimensionless)
U	superficial gas velocity ($m\ s^{-1}$)
U_{br}	single bubble rising velocity ($m\ s^{-1}$)
U_p	superficial particle velocity ($m\ s^{-1}$)
U_t	terminal particle velocity ($m\ s^{-1}$)
V	corrected velocity in transport systems ($m\ s^{-1}$)
Vol_b	gas flow into bubbles ($m^3\ s^{-1}$)

Greeks

α	corrective factor (dimensionless)
β	effectiveness factor (dimensionless)
δ	lean phase fraction in the bed (dimensionless)
ϵ	voidage fraction (dimensionless)
ϵ_f	apparent voidage fraction in bed (dimensionless)
γ	solid volume fraction relative to bubbles (dimensionless)
Ψ	slip factor, Eq. (27) (dimensionless)
η	contact efficiency (dimensionless)
μ	viscosity (kg $m^{-1}\ s^1$)
ρ	density (kg m^{-3})
τ	residence time (s)
ψ	fraction of observable bubbles in the bed, $Vol_b/((U-U_{mf})\pi d^2/4)$ (dimensionless)

Subscripts

∞	asymptotic at infinite height
a	annulus
av	averaged over section
b	bubble
bc	cloud–bubble
be	bubble–emulsion
c	core
ca	type A chocking
ce	cloud–emulsion
cl	cloud
d	riser bottom dense zone
dl	lean-dense
e	emulsion phase
f	apparent overall voidage
g	gas phase
l	lean zone
mb	minimum boiling
mf	minimum fluidisation
mp	minimum pressure drop
out	conditions at riser exit
p	particle
s	solid phase
se	onset of significant elutriation
tc	onset of turbulent fluidisation

References

[1] D. Kunii, O. Levenspiel, Fluidization Engineering, 2nd ed., Butterworth–Heinemann, London, 1991.
[2] J.R. Grace, A.A. Avidan, T.M. Knowlton (Eds.), Circulating Fluidized Beds, Blackie Academic and Professional, 1997.
[3] D. Geldart, Powder Technol. 7 (1973) 285.
[4] J.R. Grace, H. Bi, 1997, in: J.R. Grace, A.A. Avidan, T.M. Knowlton (Eds.), Circulating Fluidized Beds, Chapter 1, Blakie Academic and Professional, 1997.
[5] H.T. Bi, J.R. Grace, Int. J. Multiphase Flow 21 (1995) 1229.
[6] H.T. Bi, J.R. Grace, J. Zhu, Trans. IChemE 73 (1995) 154.
[7] H.T. Bi, J.R. Grace, J. Zhu, Int. J. Multiphase Flow 19 (1993) 1077.
[8] H.T. Bi, L.S. Fan, presented at the AIChE annual meeting, Los Angeles, CA, 1991, Paper 101e.
[9] R.D. Toomey, H.F. Johnstone, Chem. Eng. Prog. 48 (1952) 220.
[10] J.F. Davidson, D. Harrison, Fluidized Particles, Cambridge University Press, Cambridge, 1963.
[11] K. Kato, C.H. Wen, Chem. Eng. Sci. 24 (1969) 1351.
[12] C. Fryer, O.E. Potter, AIChE J. 22 (1976) 38.
[13] D. Kunii, O. Levenspiel, Ind. Eng. Chem. Res. 29 (1990) 1226.
[14] B.A. Partridge, P.N. Rowe, Trans. Inst. Chem. Eng. 44 (1966) T355.
[15] J. Werther, Chem. Eng. Sci. 47 (1992) 2457.
[16] .
[17] J. Werther, German Chem. Eng. 1 (1978) 166.
[18] A.M. Adris, C.J. Lim, J.R. Grace, Chem. Eng. Sci. 52 (1997) 1609.
[19] M.N. Bogere, Chem. Eng. Sci. 51 (1996) 603.
[20] B. Caussat, M. Hémati, J.P. Couderc, Chem. Eng. J. 58 (1995) 223.
[21] J.E. Johnsson, G.R. Grace, J.J. Graham, AIChE J. 33 (1987) 619.
[22] C. McGreavy, M.L. Lu, X.Z. Wang, E.K.T. Kam, Chem. Eng. Sci. 49 (1994) 4717.
[23] U. Pannek, L. Mleczko, Chem. Eng. Sci. 51 (1996) 3575.
[24] S.I. Reshetnikov, B.S. Balzhinimaev, V.P. Gaevoi, A.A. Ivanov, Chem. Eng. J. 60 (1995) 131.
[25] C.Y. Shiau, C.J. Lin, Chem. Eng. Sci. 48 (1993) 1299.
[26] L. Stergiou, C. Laguerie, in: D. Kunii, R. Toei (Eds.), Fluidization, Engineering Foundation, New York, 1984.
[27] J.R. Grace, Gas Fluidization Technology, Wiley, London, 1986, p. 285.
[28] J.J. van Deemter, Chem. Eng. Sci. 16 (1961) 143.
[29] L.A. Behie, P. Kehoe, AIChE J. 19 (1973) 1070.
[30] P.N. Rowe, Chem. Eng. Sci. 48 (1993) 2519.
[31] T. Miyiauchi, S. Furusaki, K. Yamada, M. Matsumura, in: G.R. Grace, J. Matsen (Eds.), Fluidization III, 1980, p. 571.
[32] M. Horio, A. Nonaka, Y. Sawa, I. Muchi, AIChE J. 32 (1986) 1466.
[33] A.M. Squires, M. Kwauk, A. Avidan, Science 230 (1985) 1329.
[34] C.O. Bolthrunis, Chem. Eng. Prog. (1989) 51.
[35] A. Arbel, Z. Huang, I.H. Rinard, R. Shinnar, A.V. Sapre, Ind. Eng. Chem. Res. 34 (1995) 1228.
[36] A. Avidan, R. Shinnar, Ind. Eng. Chem. Fundam. 29 (1990) 931.
[37] J.R. Grace, Chem. Eng. Sci. 45 (1990) 1953.
[38] M. Edwards, A. Avidan, Chem. Eng. Sci. 41 (1986) 829.
[39] M. Foka, J. Chaouki, C. Guy, D. Klvana, Chem. Eng. Sci. 49 (1994) 4269.
[40] M. Foka, J. Chaouki, C. Guy, D. Klvana, Chem. Eng. Sci. 51 (1996) 713.
[41] M. Baerns, L. Mleczko, G.J. Tjatjopoulos, I.A. Vasalos, in: A.A. Avidan (Ed.), Proceedings of the Fourth International Conference on Circulating Fluidized Beds, 1994.
[42] Y. Li, P. Wu, in: P. Basu, M. Horio, M. Hasatani (Eds.), Circulating Fluidized Bed Technology III, 1990, p. 581.
[43] R. Abed, Ind. Eng. Chem. Fundam. 24 (1985) 78.
[44] M. Horio, H. Ishii, M. Nishimuro, Powder Technol. 70 (1992) 229.

[45] D. Kunii, O. Levenspiel, Chem. Eng. Sci. 52 (1997) 2471.
[46] P. Ege, A. Grislingås, H.I. de Lasa, Chem. Eng. J. 61 (1996) 179.
[47] D. Kunii, O. Levenspiel, Powder Technol. 61 (1990) 193.
[48] K. Kato, H. Shibasaki, K. Tamura, S. Arita, C. Wang, T. Takarada, J. Chem. Eng. Jpn. 22 (1989) 130.
[49] G.S. Patience, J.S. Chaouki, F. Berruti, R. Wong, Powder Technol. 72 (1993) 31.
[50] K.S. Lim, J.X. Zhu, J.R. Grace, Int. J. Multiphase Flow 21 (1995) 141.
[51] F. Berruti, J. Chaouki, L. Godfroy, T.S. Pugsley, G.S. Patience, Can. J. Chem. Eng. 73 (1995) 579.
[52] B.J. Harris, J.F. Davidson, in: A.A. Avidan (Ed.), Circulating Fluidized Bed Technology IV, AIChE, New York, 1994.
[53] J.R. Grace, K.S. Lim, in: J.R. Grace, A.A. Avidan, T.M. Knowlton (Eds.), Circulating Fluidized Beds, Chapter 15, Blakie Academic and Professional, 1997.
[54] L.S. Fan, Chem. Eng. J. 21 (1981) 179.
[55] A. Gianetto, S. Pagliolico, G. Rovero, B. Ruggeri, Chem. Eng. Sci. 45 (1990) 2219.
[56] P. Jiang, H. Bi, R.H. Jean, L.S. Fan, AIChE J. 37 (1991) 1392.
[57] S. Pagliolico, M. Tiprigan, G. Rovero, A. Gianetto, Chem. Eng. Sci. 47 (1992) 2269.
[58] S. Ouyang, X.G. Li, O.E. Potter, Preprints of Fluidization VIII, Tours, France, 1995, p. 457.
[59] S. Ouyang, X.G. Li, O.E. Potter, AIChE J. 41 (1995) 1534.
[60] L. Marmo, G. Rovero, L. Manna, Proceedings of Fluidization VIII, Tours, France, 1996, p. 369.
[61] D.M.J. Puchyr, A.K. Mehrotra, L.A. Behie, N. Kalogerakis, Can. J. Chem. Eng. 75 (1997) 317.
[62] D. Bai, J.X. Zhu, Y. Jin, Z. Yu, Ind. Eng. Chem. Res. 36 (1997) 4543.
[63] R.J. Dry, I.N. Christensen, C.C. White, Powder Technol. 52 (1987) 243.
[64] D. Kunii, O. Levenspiel, Preprints of Fluidization VIII, Tours, France, 1995, p. 17.
[65] S. Furusaki, T. Kikuchi, T. Miyiauchi, AIChE J. 22 (1976) 354.
[66] R.J. Dry, C.C. White, Powder Technol. 70 (1992) 277.
[67] C.H.M. Brereton, J.R. Grace, J. Yu, in: P. Basu, J.F. Large (Eds.), Circulating Fluidized Bed Technology II, 1988, p. 307.
[68] D. Bai, J. Yong, Y. Zhiquing, Third China–Japan Symposium, Beijing, China, 1988, p. 155.
[69] C.C. White, R.J. Dry, O.E. Potter, Circulating Fluidized Bed Technology VII, 1992, p. 265.
[70] G.S. Patience, J.S. Chaouki, Chem. Eng. Sci. 48 (1993) 3195.
[71] H. Kagawa, H. Mineo, R. Yamazaki, K. Yoshida, in: P. Basu, M. Horio, M. Hasatani (Eds.), Circulating Fluidized Bed Technology III, 1990, p. 551.
[72] T.S. Pugsley, F. Berruti, Chem. Eng. Sci. 51 (1996) 2751.
[73] H.T. Bi, P. Jiang, R.H. Jean, L.S. Fan, Chem. Eng. Sci. 47 (1992) 3113.
[74] D.M.J. Puchyr, A.K. Mehrotra, L.A. Behie, N. Kalogerakis, Chem. Eng. Sci. 51 (1996) 5251.
[75] T.S. Pugsley, F. Berruti, U. Pannek, L. Mleczko, Fifth International Conference on Circulating Fluidized Beds, Beijing, China, 1996.
[76] T.S. Pugsley, S. Malcus, Ind. Eng. Chem. Res. 36 (1997) 4567.
[77] J. Werther, Proceedings of the IV Conference on Circulating Fluidized Beds, Somerset, USA, 1994, p. 1.
[78] T.S. Pugsley, F. Berruti, Powder Technol. 89 (1996) 57.
[79] W.T. Zhang, Y. Tung, F. Johnsson, Chem. Eng. Sci. 46 (1991) 3045.
[80] M.J. Rhodes, X.S. Wang, H. Cheng, T. Hirama, Chem. Eng. Sci. 47 (1992) 1635.
[81] M. Kruse, J. Werther, Chem. Eng. Process. 34 (1995) 185.
[82] C. Martin, C. Derouin, P. Turlier, M. Forissier, G. Wild, J.R. Bernard, Chem. Eng. Sci. 47 (1992) 2319.
[83] C. Martin, P. Turlier, J.R. Bernard, G. Wild, Powder Technol. 70 (1992) 249.
[84] W.C. Yang, Z. Huang, L. Zhao, Fluidization IV, eng Foundation, New York, 1984, p. 145.
[85] R. Bader, J. Findlay, T. Knowlton, in: P. Basu, J.F. Large (Eds.), Circulating Fluidized Bed Technology II, 1988, p. 123.
[86] J. Werther, E.U. Hartge, M. Kruse, in: O.E. Potter, D.J. Nicklin (Eds.), Fluidization VII, Engineering Foundation, New York, 1992, p. 257.
[87] C. Adams, in: P. Basu, J.F. Large (Eds.), Circulating Fluidized Bed Technology II, 1988, p. 299.
[88] G. Amos, M.J. Rhodes, H. Mineo, Chem. Eng. Sci. 48 (1993) 943.
[89] P. Gayan, L.F. de Diego, J. Adanez, Powder Technol. 94 (1997) 163.
[90] C. Derouin, D. Nevicato, M. Forissier, G. Wild, Ind. Eng. Chem. Res. 36 (1997) 4504.
[91] H. Schoenfelder, M. Kruse, J. Werther, AIChE J. 42 (1996) 1875.
[92] H. Schoenfelder, M. Kruse, J. Werther, Proceedings of the Fifth International Conference on Circulating Fluidized Bed Reactors, Beijing, China, 1996.
[93] M. Flinger, P.H. Schipper, A.V. Sapre, F.J. Krambeck, Chem. Eng. Sci. 49 (1994) 4269.
[94] J.L. Sinclair, in: J.R. Grace, A.A. Avidan, T.M. Knowlton (Eds.), Circulating Fluidized Beds, Chapter 5, Blakie Academic and Professional, 1997.
[95] D. Gidaspow, Multiphase Flow and Fluidization, Academic Press, San Diego, 1994.
[96] T. Hyppänen, Y.Y. Lee, A. Rainio, in: P. Basu, M. Horio, M. Hasatani (Eds.), Circulating Fluidized Bed Technology III, 1990, p. 563.
[97] U. Arena, R. Chirone, M. D'Amore, M. Miccio, Powder Technol. 82 (1995) 301.
[98] H. Schoenfelder, J. Hinderer, J. Werther, F.J. Keil, Chem. Eng. Sci. 49 (1994) 5377.
[99] H. Schoenfelder, J. Werther, J. Hinderer, F.J. Keil, AIChE Symp. Ser. 90 (1994) 92.

[100] K.B. Mathur, J.C. Lim, Chem. Eng. Sci. 29 (1974) 789.
[101] N. Piccinini, J.R. Grace, K.B. Mathur, Chem. Eng. Sci. 34 (1979) 1257.
[102] G. Rovero, N. Piccinini, J.R. Grace, N. Epstein, Chem. Eng. Sci. 38 (1983) 557.
[103] G. Rovero, C.M.H. Brereton, N. Epstein, J.R. Grace, L. Casalegno, N. Piccinini, Can. J. Chem. Eng. 61 (1983) 289.
[104] B.D. Hook, H. Littman, M.M. Morgan, Can. J. Chem. Eng. 70 (1992) 966.
[105] K.J. Smith, Y. Arkun, H. Littman, Chem. Eng. Sci. 37 (1982) 567.